NFN - Nationales Forschungsnetzwerk

Geometry + Simulation

http://www.gs.jku.at

Approximately C^1-smooth Isogeometric Functions on Two-Patch Domains

Agnes Seiler and Bert Jüttler

G+S Report No. 77

January 2019

Der Wissenschaftsfonds.

JOHANNES KEPLER UNIVERSITY LINZ

Approximately C^1-smooth Isogeometric Functions on Two-Patch Domains

Agnes Seiler, Bert Jüttler

Abstract Motivated by the promising recent results concerning the construction of smooth isogeometric functions on multi-patch domains on bilinearly parameterized domains [14] or reparameterizations of more general domains [5], which, however, impose quite restrictive assumptions on the underlying domain, we propose two approaches to construct spaces $G_h^{1,\varepsilon}$ of approximately C^1-smooth isogeometric functions on general two-patch domains. The main idea is to work with C^0-continuous functions and to bound the jump of their gradients across the interface between neighboring patches. The constructions are based on two suitably chosen bilinear forms $\mathcal{B}_1$ and $\mathcal{B}_2$ and their eigenstructures, which lead to different bounds on the gradient jumps, respectively. We show that while the gradient jumps of the functions based on $\mathcal{B}_1$ fulfill a stricter bound, the functions themselves do not realize optimal convergence rates. Numerical experiments suggest that the functions based on $\mathcal{B}_2$ reach the optimal approximation order for solving second order problems. Furthermore, they are smooth enough to solve higher order problems such as the biharmonic equation. However, the bound on their gradient jump is mesh-size dependent.

1 Introduction

Isogeometric Analysis, introduced in 2005 by Hughes et al. [6], is an approach to numerical simulation via partial differential equations (PDEs). The computational domain is represented by a spline parameterization, which is called the geometry

Agnes Seiler
Doctoral Program Computational Mathematics, Johannes Kepler University Linz, Austria. e-mail: agnes.seiler@dk-compmath.jku.at

Bert Jüttler
Institute of Applied Geometry, Johannes Kepler University Linz, Austria. e-mail: bert.juettler@jku.at

mapping. The discretization relies on isogeometric functions, which serve as test functions in the weak form of the problem. They are obtained by concatenating the basis functions that contribute to the parameterization of the geometry with the inverse geometry mapping. Hence, Isogeometric Analysis (IgA) does not need a triangulation of the domain. Since it directly uses a spline parameterization to define the discretization, it is said to close the gap between the CAD representation of the geometry and numerical analysis [6].

Another advantage of IgA consists is the increased smoothness of the discretization compared to standard finite elements. Within the patches, isogeometric functions are typically C^{p-1} smooth. This facilitates the discretization of higher order problems. While simple physical domains can be parameterized by a single geometry map, more complicated ones will be represented as a collection of several patches, each of which with its own parameterization. In this case, the multi-patch structure of the domain has to be taken into account, since the isogeometric functions are not automatically smooth across patch interfaces. Thus, appropriate coupling methods are required.

Standard coupling methods from the finite element literature carry over to multi-patch isogeometric discretizations. These methods work with broken Sobolev spaces, where weak differentiability across patch interfaces is not guaranteed. Suitable coupling terms are added to the weak form of a partial differential equation. For instance, the mortar method [2, 3], Nitsche Mortaring [16, 19] or the discontinuous Galerkin method [15, 17] perform the coupling via average and jump terms. Those terms need to be adapted to the order of the problem. While it suffices to consider the jump of function values for second order problems, fourth order problems require to take the difference of the normal derivatives into account. More generally, via the relation between a coercive bilinear form of an elliptic problem and its equivalent quadratic optimization problem, suitable methods from non-linear optimization can be applied to the coupling problem [8].

This paper explores a different approach, which is based on approximately smooth isogeometric test functions on the entire domain. Consequently, no modification of the variational form is required.

The coupling of isogeometric discretization across patch interfaces recently attracted substantial interest:

- C^0-coupling of isogeometric functions can be performed easily by identifying the coefficients of neighboring basis functions along an interface.
- The construction of C^1-smooth test functions, which are useful for higher order problems, is considerably more complicated. Recent results rely on the relation between geometric continuity of a graph surface and the smoothness of the associated functions [7, 14]. However, C^1-constructions are based on certain assumptions about the parameterization of the underlying domain, which are needed to ensure sufficient flexibility of the resulting discretizations. For instance, in [9, 14], the authors use bilinear or bilinear-like parameterizations. A reparameterization is needed for more general domains [5, 10]. A numerical approach to the computation of C^1-smooth discretization is presented in [4].

- These results have partially been extended to C^2-smooth isogeometric discretizations [11, 12, 13].

In order to avoid the limitation to bilinear-like parameterizations, we relax the construction by considering approximate C^1 smoothness of isogeometric functions on multi-patch domains. This enables us to generate function spaces on general (not bilinear-like) domains. Our construction is based on suitably chosen bilinear forms. More precisely, we explore two different forms and obtain two different function spaces. Starting from globally C^0-smooth functions, we provide bounds on the gradient jump of the corresponding approximately C^1-smooth isogeometric functions.

The remainder of this paper is organized as follows: Section 2 introduces the notation and the two different bilinear forms $\mathcal{B}_1$ and $\mathcal{B}_2$. The next section describes the construction of a space of approximately C^1-smooth isogeometric functions based on $\mathcal{B}_1$ and investigates its properties. In particular, we observe that the resulting space is not guaranteed to contain the trivially smooth functions. In order to address this deficiency, Section 4 describes another construction, which is based on the simplified bilinear form $\mathcal{B}_2$. Section 5 is devoted to numerical experiments concerning the approximation power and the dimension of the spaces. In particular, we will provide experiments suggesting that the functions we construct are smooth enough to solve fourth-order problems. Finally, we conclude the paper.

2 Preliminaries

We consider a planar two-patch domain $\Omega = \Omega^1 \cup \Omega^2 \subseteq \mathbb{R}^2$ with interface Γ between the individual patches Ω^1 and Ω^2, as depicted in Figure 1. It is parameterized by a

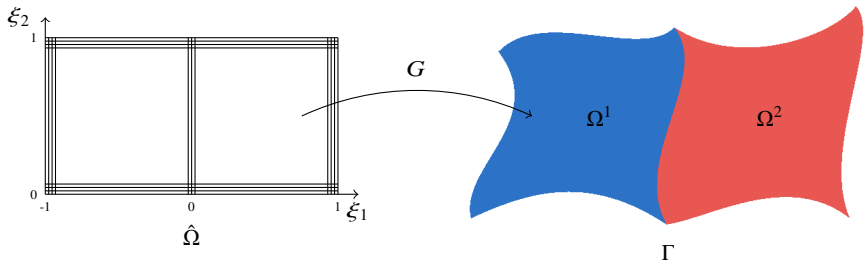

Fig. 1 Two patch domain Ω parameterized by a bicubic geometry map G. The knot vectors are given by $[-1,-1,-1,-1,0,0,0,1,1,1,1] \times [0,0,0,0,1,1,1,1]$.

tensor-product B-spline mapping G via

$$G : \hat{\Omega} \to \Omega : (\xi_1, \xi_2) \mapsto \sum_{i \in \mathcal{I}} P_i \beta_i(\xi_1, \xi_2), \quad (\xi_1, \xi_2) \in \hat{\Omega} = [-1,1] \times [0,1], \quad (1)$$

where $P_i \in \mathbb{R}^2$ are control points and β_i are tensor-product B-splines of bidegree (p_1, p_2) with index set $\mathcal{I}$, defined by open knot vectors Ξ_1, Ξ_2 with maximal knot span sizes h_1, h_2 in ξ_1 and ξ_2 direction, respectively. We set $h = \max\{h_1, h_2\}$. The multiplicities of the inner knots do not exceed $p - 1$, except for the knot 0 in Ξ_1, which appears p times. The simplest instance of the knot configuration is visualized in Figure 1. The patch interface is $\Gamma = G(\{0\} \times [0,1])$. The associated isogeometric basis functions

$$b_i(\boldsymbol{x}) = \left(\beta_i \circ G^{-1}\right)(\boldsymbol{x}),\ i \in \mathcal{I} \tag{2}$$

are collected in the vector

$$\boldsymbol{b}(\boldsymbol{x}) = (b_i(\boldsymbol{x}))_{i \in \mathcal{I}} \tag{3}$$

and span the isogeometric discretization space

$$\mathcal{V}_h = \operatorname{span}\{b_i : i \in \mathcal{I}\} \subseteq C^0(\Omega). \tag{4}$$

Finally we recall the definition of the jump operator

$$[f] = f^1|_\Gamma - f^2|_\Gamma,$$

which is defined for any function $f \in L^2(\Omega)$ with

$$f^1 = f|_{\Omega^1} \in H^1(\Omega^1), \quad f^2 = f|_{\Omega^2} \in H^1(\Omega^2).$$

We will use two different bilinear forms in order to construct approximately C^1-smooth isogeometric functions on Ω. The first one is given by

$$\mathcal{B}_1 : \mathcal{V}_h \times \mathcal{V}_h \to \mathbb{R} : (f,g) \mapsto \varepsilon \int_\Omega f(\boldsymbol{x}) g(\boldsymbol{x}) d\boldsymbol{x} - \int_\Gamma [\nabla f(\boldsymbol{x})]^T [\nabla g(\boldsymbol{x})] d\boldsymbol{x} \tag{5}$$

and depends on a positive parameter ε. The second one takes the form

$$\mathcal{B}_2 : \mathcal{V}_h \times \mathcal{V}_h \to \mathbb{R} : (f,g) \mapsto \int_\Gamma [\nabla f(\boldsymbol{x})]^T [\nabla g(\boldsymbol{x})] d\boldsymbol{x}. \tag{6}$$

More precisely, our aim is to construct isogeometric functions with a bounded gradient jump $\|[\nabla f]\|_{L^2(\Gamma)}$, and the bilinear forms $\mathcal{B}_1$ and $\mathcal{B}_2$ are designed with this objective in mind. For the first one, a suitable value of ε has to be chosen in advance. It controls the magnitude of the bound. The spaces of approximately smooth isogeometric functions obtained by using $\mathcal{B}_1$ and $\mathcal{B}_2$ have different properties, although the constructions themselves are quite similar.

3 Results for $\mathcal{B}_1$

We show that the bilinear form $\mathcal{B}_1$ yields a mesh-size independent bound on the gradient jump. However, we will also see that this space lacks optimal approximation power.

3.1 Construction of Approximately Smooth Functions

We consider functions $f, g \in \mathcal{V}_h$ with

$$f(\boldsymbol{x}) = u^T \boldsymbol{b}(\boldsymbol{x}), g(\boldsymbol{x}) = v^T \boldsymbol{b}(\boldsymbol{x}), \tag{7}$$

with coefficient vectors $u, v \in \mathbb{R}^{|\mathcal{I}|}$. Consequently, $\mathcal{B}_1(f,g)$ can be rewritten in matrix-vector-form as

$$\mathcal{B}_1(f,g) = u^T(\varepsilon M - Q)v, \tag{8}$$

where

$$M = (m_{i,j})_{i,j\in\mathcal{I}} \text{ with } m_{i,j} = \int_\Omega b_i(\boldsymbol{x}) b_j(\boldsymbol{x}) d\boldsymbol{x} \tag{9}$$

and

$$Q = (q_{i,j})_{i,j\in\mathcal{I}} \text{ with } q_{i,j} = \int_\Gamma [\nabla b_i(\boldsymbol{x})]^T [\nabla b_j(\boldsymbol{x})] d\boldsymbol{x}, \tag{10}$$

as confirmed by a short computation. The matrices M and Q are symmetric positive semi-definite, as

$$u^T M u = \|f\|^2_{L^2(\Omega)} \geq 0 \tag{11}$$

and

$$u^T Q u = \|[\nabla f]\|^2_{L^2(\Gamma)} \geq 0. \tag{12}$$

Now let $0 \leq \lambda^1 \leq \ldots \leq \lambda^n$ be the non-negative eigenvalues of $\varepsilon M - Q$ in ascending order and let $c^1, \ldots, c^n$ be the corresponding eigenvectors, $n \leq |\mathcal{I}|$. The eigenvectors satisfy

$$(c^k)^T c^\ell = 0 \text{ and } (c^k)^T c^k = 1 \text{ for } k \neq \ell, 1 \leq k, \ell \leq n, \tag{13}$$

possibly after performing the Gram-Schmidt orthonormalization, if multiple eigenvalues are present.

We define

$$\begin{aligned} G_h^{1,\varepsilon} &:= \operatorname{span}\left\{ \sum_{i\in\mathcal{I}} c_i^k b_i(\boldsymbol{x}) : k = 1, \ldots, n \right\} \\ &= \left\{ \sum_{i\in\mathcal{I}} d_i b_i(\boldsymbol{x}) : d \in \operatorname{span}\left\{c^1, \ldots c^n\right\} \right\}. \end{aligned} \tag{14}$$

as the *space of approximately C^1-smooth isogeometric functions*.

3.2 Properties of the Function Space

By construction, $G_h^{1,\varepsilon}$ is a linear space. As an immediate consequence from its definition, we obtain a mesh-size independent bound on the gradient jump.

We denote by $\boldsymbol{C} \in \mathbb{R}^{|\mathcal{I}|\times n}$ the matrix containing the eigenvectors $c^1, \ldots, c^n$ as column vectors.

Proposition 1 *The gradient jump of any function $f = (\boldsymbol{C}d)^T \boldsymbol{b} \in G_h^{1,\varepsilon}$ with $d \in \mathbb{R}^n$ can be bounded by*

$$\|[\nabla f]\|^2_{L^2(\Gamma)} \leq \varepsilon \|f\|^2_{L^2(\Omega)}. \tag{15}$$

Proof We use (11) and (12) and obtain

$$\begin{aligned}
\varepsilon\|f\|^2_{L^2(\Omega)} - \|[\nabla f]\|^2_{L^2(\Gamma)} &= (\boldsymbol{C}d)^T(\varepsilon M - Q)(\boldsymbol{C}d) \\
&= d^T \boldsymbol{C}^T(\varepsilon M - Q)\boldsymbol{C}d \\
&= d^T \operatorname{diag}\left(\lambda^1, \ldots, \lambda^n\right) d \\
&= \lambda^1 d_1^2 + \ldots + \lambda^n d_n^2 \geq 0,
\end{aligned}$$

where the last inequality holds because we only consider non-negative eigenvalues λ_i. □

The space $G_h^{1,\varepsilon}$ based on $\mathcal{B}_1$ does not necessarily contain the trivially smooth isogeometric functions b_i^k with

$$\nabla b_i^k|_\Gamma = \mathbf{0}.$$

We will refer to these functions as *off-interface basis functions*. Since they are constantly zero across the interface Γ, their gradient jumps across Γ are zero as well. However, their coefficient vectors with respect to the basis $\boldsymbol{b}$, which are the canonical unit vectors in $\mathbb{R}^{|\mathcal{I}|}$, are not necessarily eigenvectors of $\varepsilon M - Q$. As we shall see in Section 5, the functions in $G_h^{1,\varepsilon}$ do not possess the same approximation power as the full space of isogeometric functions.

4 Results for $\mathcal{B}_2$

We study another bilinear form in order to ensure the existence of trivially smooth functions in the resulting space of approximately smooth isogeometric functions. However, in this case we cannot expect to obtain an estimate of $\|[\nabla f]\|_{L^2(\Gamma)}$ that is independent of the mesh size.

4.1 Construction of Approximately Smooth Functions

The modified space $\hat{G}_h^{1,\varepsilon}$ is constructed analogously to the procedure described in Section 3.1. Recall that $\mathcal{B}_2(f,f)$ can equivalently be written as

$$\mathcal{B}_2(f,f) = u^T Q u$$

for

$$f = u^T \boldsymbol{b} \in \mathcal{V}_h, \quad u \in \mathbb{R}^{|\mathcal{I}|}.$$

As explained before, the matrix Q is symmetric positive semi-definite. We choose a positive value ε. Let $\hat{\lambda}^1 \leq \ldots \leq \hat{\lambda}^{\hat{n}} \leq \varepsilon$ be the eigenvalues of Q that are bounded by ε and let $\hat{c}^1, \ldots, \hat{c}^{\hat{n}}$ be the corresponding orthonormalized eigenvectors, $\hat{n} \leq |\mathcal{I}|$. We define

$$\hat{G}_h^{1,\varepsilon} := \operatorname{span}\left\{ \sum_{i \in \mathcal{I}} \hat{c}_i^k b_i : k = 1, \ldots, \hat{n} \right\}. \tag{16}$$

4.2 Properties of the Function Space

Again, by construction, $\hat{G}_h^{1,\varepsilon}$ is a linear space. Moreover, all trivially smooth isogeometric functions f, i.e., the off-interface basis functions as well as constant and linear functions (which are contained in the space of isogeometric functions, due to use of the isoparametric principle), fulfill

$$\mathcal{B}(f,f) = 0.$$

Since the matrix Q is symmetric positive semi-definite, this implies that the coefficient vector of f is an element of the kernel of Q. Consequently, the corresponding coefficient vector is an eigenvector to the eigenvalue 0 of Q. Since we set $\varepsilon > 0$, all elements in the kernel will also be elements of $\hat{G}_h^{1,\varepsilon}$. This is independent of the mesh size h. As we will see, the inclusion of these functions in $\hat{G}_h^{1,\varepsilon}$ is important to achieve optimal convergence.

Subsequently, we bound the gradient jump of functions in $\hat{G}_h^{1,\varepsilon}$. We denote by $\hat{\boldsymbol{C}} \in \mathbb{R}^{|\mathcal{I}| \times \hat{n}}$ the matrix containing the eigenvectors $\hat{c}^1, \ldots, \hat{c}^{\hat{n}}$ of Q as column vectors. Let $f \in \hat{G}_h^{1,\varepsilon}$, i.e. we set

$$f(\boldsymbol{x}) = (\hat{\boldsymbol{C}} d)^T \boldsymbol{b}(\boldsymbol{x}) \tag{17}$$

with $d \in \mathbb{R}^n$.

Theorem 1 *Let the knot vectors Ξ_1, Ξ_2 be quasi-uniform. Then all functions $f \in \hat{G}_h^{1,\varepsilon}$ satisfy*

$$\|[\nabla f]\|_{L^2(\Gamma)}^2 \leq \varepsilon \frac{C}{h^2} \|f\|_{L^2(\Omega)}^2 \tag{18}$$

for a constant C that depends on the maximal spline degree p and the geometry mapping G, but not on the maximal mesh size h.

Proof Let $f = (\hat{\boldsymbol{C}}d)^T \boldsymbol{b} \in G_h^{1,\varepsilon}$ as denoted above. Then we have

$$\begin{aligned}
\|[\nabla f]\|^2_{L^2(\Gamma)} &= (\hat{\boldsymbol{C}}d)^T Q(\hat{\boldsymbol{C}}d) = d^T \hat{\boldsymbol{C}}^T Q \hat{\boldsymbol{C}} d \\
&= d^T \operatorname{diag}\left(\hat{\lambda}^1, \ldots, \hat{\lambda}^{\hat{n}}\right) d \\
&= \hat{\lambda}^1 d_1^2 + \ldots + \hat{\lambda}^{\hat{n}} d_{\hat{n}}^2 \\
&\leq \varepsilon \sum_{i=1}^{\hat{n}} d_i^2 = \varepsilon \|d\|_2^2 = \varepsilon \|\hat{\boldsymbol{C}} d\|_2^2,
\end{aligned}$$

where the last equality holds because $\hat{\boldsymbol{C}}$ is an orthogonal matrix.

Next, we use the stability of tensor-product B-spline bases $\{\beta_i\}_{i\in\mathcal{I}}$ [18] with stability constant D_p^2, where $p = \max\{p_1, p_2\}$ and get

$$\|[\nabla f]\|^2_{L^2(\Gamma)} \leq \varepsilon \|\hat{\boldsymbol{C}} d\|_2^2 \leq \varepsilon D_p^4 \frac{1}{h^2} \left\| \sum_{i\in\mathcal{I}} (\hat{\boldsymbol{C}}d)_i \beta_i \right\|^2_{L^2(\hat{\Omega})}. \tag{19}$$

We rewrite β_i in terms of the push-forward $b_i \circ G$ and obtain

$$\|[\nabla f]\|^2_{L^2(\Gamma)} \leq \varepsilon D_p^4 \frac{1}{h^2} \left\| \sum_{i\in\mathcal{I}} (\hat{\boldsymbol{C}}d)_i \, (b_i \circ G) \right\|^2_{L^2(\hat{\Omega})}, \tag{20}$$

which again can be rewritten and summarized as

$$\begin{aligned}
\|[\nabla f]\|^2_{L^2(\Gamma)} &\leq \varepsilon D_p^4 \frac{1}{h^2} \left\| \left(\sum_{i\in\mathcal{I}} (\hat{\boldsymbol{C}}d)_i b_i \right) \circ G \right\|^2_{L^2(\hat{\Omega})} \\
&= \varepsilon D_p^4 \frac{1}{h^2} \|f \circ G\|^2_{L^2(\hat{\Omega})}.
\end{aligned} \tag{21}$$

Now we transform the integral $\int_{\hat{\Omega}} (f \circ G)^2$ on $\hat{\Omega}$ to an integral on Ω, which yields

$$\|[\nabla f]\|^2_{L^2(\Gamma)} \leq \varepsilon D_p^4 \frac{1}{h^2} \|\det \nabla(G)^{-1}\|_{L^\infty(\Omega)} \|f\|^2_{L^2(\Omega)}. \tag{22}$$

Finally we set

$$C(p, G) = D_p^4 \cdot \left\| \det \nabla(G)^{-1} \right\|_{L^\infty(\Omega)}.$$

This concludes the proof. □

This result resembles standard inverse inequalities for isogeometric functions, which can be found in [1], apart from the power of h and the factor ε, which is chosen in advance. If we chose $\varepsilon \in O(h^2)$, we can eliminate the mesh-size depen-

dence in the bound of the gradient jump. However, smaller values of ε lead to fewer functions in $\hat{G}_h^{1,\varepsilon}$, which we will discuss in the following section.

5 Numerical Examples

We consider least squares approximation, the Poisson problem, and the biharmonic equation on a two-patch domain. In this context we are interested in the approximation power of $G_h^{1,\varepsilon}$ and $\hat{G}_h^{1,\varepsilon}$. Furthermore we will study the number of interface basis functions under uniform h-refinement.

5.1 Approximation Power

Throughout the remainder of this section, all errors are measured patch-wisely and then summed up, e.g. we refer to

$$\|f_{\text{approx}}|_{\Omega^1} - f_{\text{exact}}|_{\Omega^1}\|_{H^1(\Omega^1)} + \|f_{\text{approx}}|_{\Omega^2} - f_{\text{exact}}|_{\Omega^2}\|_{H^1(\Omega^2)}$$

as the H^1 error and to

$$\|f_{\text{approx}}|_{\Omega^1} - f_{\text{exact}}|_{\Omega^1}\|_{H^2(\Omega^1)} + \|f_{\text{approx}}|_{\Omega^2} - f_{\text{exact}}|_{\Omega^2}\|_{H^2(\Omega^2)}$$

as the H^2 error of f_{approx}. The patch-wise splitting is not necessary for the L^2 error, as $G_h^{1,\varepsilon} \subseteq L^2(\Omega)$ and $\hat{G}_h^{1,\varepsilon} \subseteq L^2(\Omega)$.

Least Squares Approximation

We start with an example that identifies the limitations of the space $G_h^{1,\varepsilon}$, which is based on the bilinear form $\mathcal{B}_1$. Figure 2 shows the function

$$f_{\text{exact}}(x, y) = 3xy \exp(-x) \sin(\pi y) \tag{23}$$

which we approximate on a two-patch domain by functions in $G_h^{1,\varepsilon}$. The domain coincides with the one shown in Figure 1. We solve the constrained least squares fitting problem

$$\min_{f \in G_h^{1,\varepsilon}} \|f - f_{\text{exact}}\|^2_{L^2(\Omega)}.$$

The parameter ε was set to 0.5. The relative L^2 and H^1 errors are depicted in the left plot of Figure 3. After some refinement steps, no significant reduction of the error is achieved. Considering the distribution of the error values in the last refinement step, shown in Figure 3, right, we note that the largest errors occur close to the interface

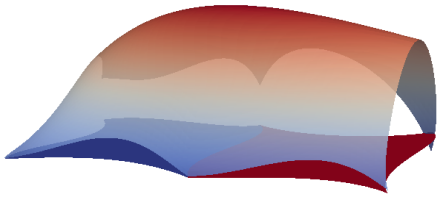

Fig. 2 Bicubically parameterized domain (see Fig. 1) and transparent plot of the exact solution $3xy\exp(-x)\sin(\pi y)$.

and in the back corners. This is a possible indicator that the corresponding corner basis functions are not present in $G_h^{1,\varepsilon}$.

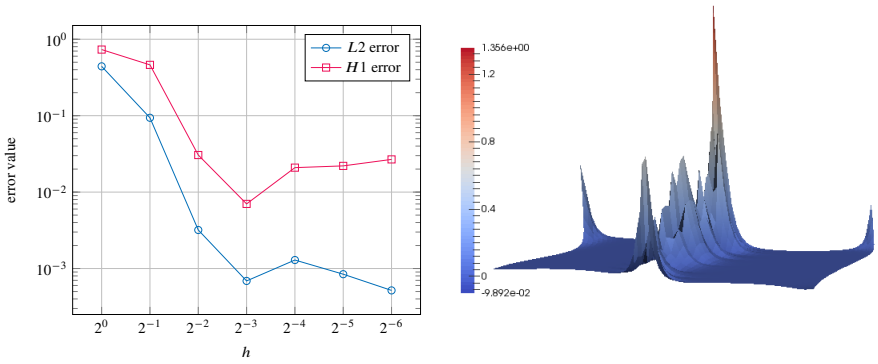

Fig. 3 Least squares approximation with functions in $G_h^{1,\varepsilon}$ with $\varepsilon = 0.5$. Left: relative L^2 and H^1 error for the approximate solution of degree 3. Right: L^2 error values at the finest discretization step (scaled by factor 100).

Consequently, we consider only the space $\hat{G}_h^{1,\varepsilon}$ based on the bilinear form $\mathcal{B}_2$. The following experiment shows that - in contrast to the previous approach - the functions in $\hat{G}_h^{1,\varepsilon}$ maintain the full approximation power.

Again, we choose $\varepsilon = 0.5$ and approximate the same function (23) on the same domain as before. We use a uniform h-refinement strategy. The relative L^2 and H^1 error values and the respective convergence rates are shown in Figure 4, top left and top right. A comparison with the reference slopes shows that the functions in $\hat{G}_h^{1,\varepsilon}$ maintain the optimal convergence rates of $p+1$ and p for the L^2 and the H^1 error, respectively.

At the finest level of refinement we used 8,840 (9,111) basis functions of degree 3 (4) with mesh size 2^{-6}. Note that this number of basis functions is slightly less than the number of original tensor-product B-splines, which is 8,978 (9,248) for degree 3 (4).

The bottom plot in Figure 4 depicts the solution using 8,840 basis functions of degree 3 as a patch-wise plot with added flat shading. These effects highlight the smoothness of the solution across the curved interface.

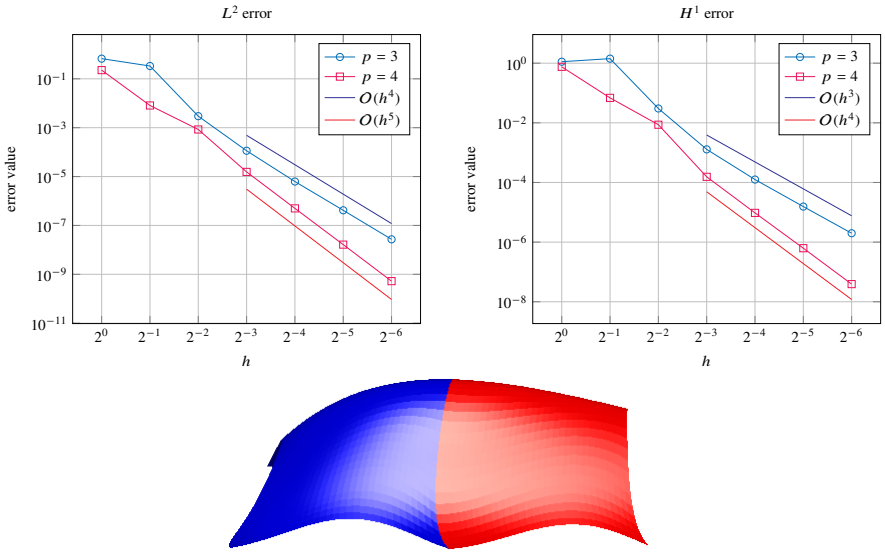

Fig. 4 Least squares approximation with functions in $\hat{G}_h^{1,\varepsilon}$ with $\varepsilon = 0.5$. Relative L^2 (top left) and H^1 (top right) error of the solution to the fitting problem on the bi-cubic domain, see Figure 1. Bottom: patch-wise representation of the solution with 8,840 basis functions of degree three with flat shading.

Poisson Problem

Solving the Poisson equation leads to very similar results. We consider the discretized weak form:

$$\text{Find } u \in \hat{G}_{h,0}^{1,\varepsilon} \text{ such that } \int_\Omega \nabla u(\boldsymbol{x}) \nabla v(\boldsymbol{x}) d\boldsymbol{x} = \int_\Omega f(\boldsymbol{x}) v(\boldsymbol{x}) d\boldsymbol{x} \quad \forall v \in \hat{G}_{h,0}^{1,\varepsilon}, \tag{24}$$

where $\hat{G}_{h,0}^{1,\varepsilon} = \{u \in \hat{G}_h^{1,\varepsilon} : u|_{\partial\Omega} = 0\}$. The zero Dirichlet boundary conditions are imposed strongly in the test function space. Again we set the threshold ε to 0.5. The exact solution is given by

$$\begin{aligned} u(x,y) = 40&(0.25x + 0.75 - y)(-0.25x + 1.25 - y) \\ &(-0.25x + 0.25 - y)(0.25x - 0.25 - y)\sin(0.5\pi x). \end{aligned}$$

The physical domain Ω consists of two patches with a curved interface, see Figure 5, left. It is biquadratically parametrized. The solution to (24) is found by means of a Galerkin method. Figure 5, right, shows its solution for 2,048 degrees of freedom with element size 2^{-5}. The patch-wise plot with the flat shading effect emphasizes that the solution is smooth in the area of the interface.

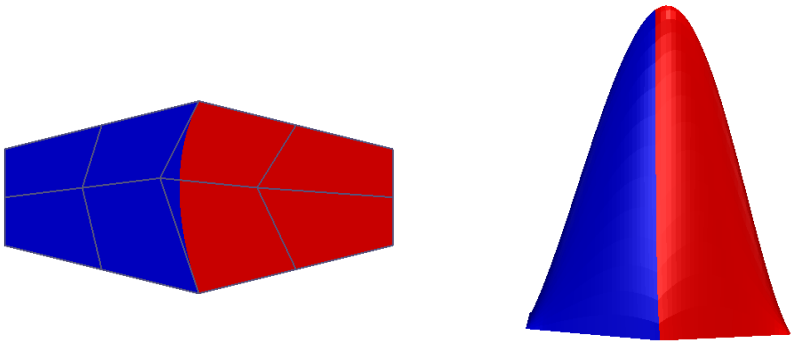

Fig. 5 Poisson problem (24). Left: Domain Ω and its control net. Right: Patch-wise plot of the solution with 2,048 basis functions of degree two in $\hat{G}_h^{1,\varepsilon}$ for $\varepsilon = 0.5$ with flat shading.

The behavior of the relative L^2 and the H^1 error are shown in Figure 6, left and right, respectively. We see that in both cases and for the tested degrees two, three and four of test functions we realize optimal convergence rates. This is consistent with the L^2 approximation results.

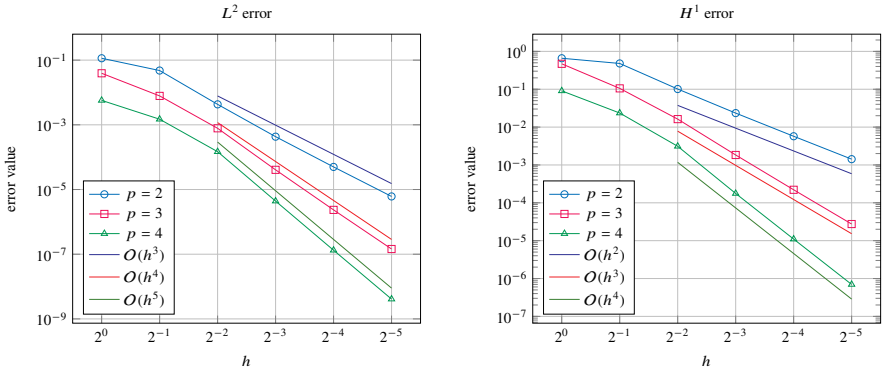

Fig. 6 Poisson problem (24). Relative L^2 (left) and H^1 error (right) of the approximate solution for basis functions of different degrees in $\hat{G}_h^{1,\varepsilon}$ for $\varepsilon = 0.5$.

Biharmonic Equation

The examples shown previously did not require C^1-smooth basis functions. Consequently, the approximately smooth functions we presented did not exhibit any advantage over standard C^0-smooth isogeometric functions (which can be constructed by identifying the corresponding degrees of freedom along the interface), except for the fact that we used slightly less basis functions. We now consider a fourth-order equation, where the bilinear form governing the weak formulation cannot be evaluated for only C^0-smooth functions. The following examples demonstrate that - depending on the value of the parameter ε that controls the magnitude of the jump - approximately smooth functions are suitable for solving such a higher-order problem and even to maintain full approximation power with respect to the L^2, H^1 and H^2 error.

We consider the discretized weak form of the biharmonic equation:

$$\text{Find } u \in \hat{G}^{1,\varepsilon}_{h,\mathbf{0}} \text{ such that } \int_\Omega \Delta u(\boldsymbol{x}) \Delta v(\boldsymbol{x}) d(\boldsymbol{x}) = \int_\Omega f(\boldsymbol{x}) v(\boldsymbol{x}) \quad \forall v \in \hat{G}^{1,\varepsilon}_{h,\mathbf{0}}, \quad (25)$$

where $\hat{G}^{1,\varepsilon}_{h,\mathbf{0}} = \{u \in \hat{G}^{1,\varepsilon}_h : u|_{\partial\Omega} = (\nabla u \cdot n)|_{\partial\Omega} = 0\}$. Again, we impose the boundary conditions strongly in the test function space and solve (25) by means of the Galerkin method. The right-hand side f is obtained from the exact solution $(1 - \cos(2\pi x))(1 - \cos(2\pi y))$. The domain Ω is a square, which is split into two patches with a curved interface, see Figure 7, left. Figure 7, right, depicts the solution for 2101 basis functions of degree four and element size $h = 2^{-5}$ for $\varepsilon = h^2$. The shading demonstrates the smoothness of the solution across the interface in the patch-wise plot.

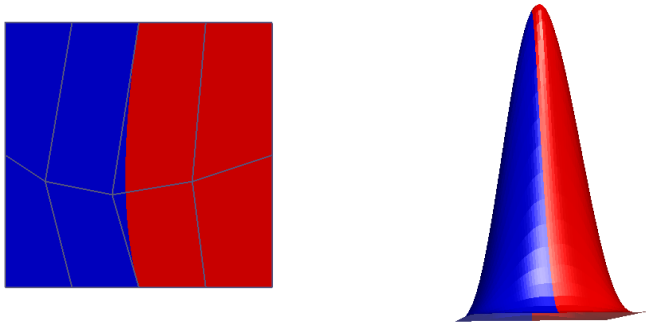

Fig. 7 Biharmonic equation (25): Domain with its control net (left) and patch-wise plot of the solution with shading (right) for 2101 basis functions of degree four in $\hat{G}^{1,\varepsilon}_h$ with $\varepsilon = h^2$.

We consider the decay of the relative error for different degrees of the basis functions, starting with degree $p = 3$. The plots in Figure 8 show that the optimal ap-

proximation order with respect to the L^2 (left) and H^2 (right) norm is reached for $\varepsilon = C \cdot h^k$ for $k \leq 2$, but not for $k = 3$.

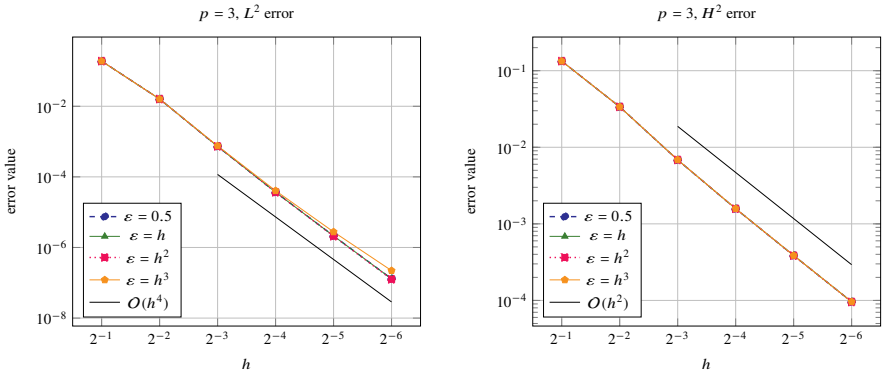

Fig. 8 Biharmonic equation (25): Relative L^2 (left) and H^2 (right) errors of the approximate solution for basis functions of degree three in $\hat{G}_h^{1,\varepsilon}$ for four choices of ε.

The situation is slightly different for $p = 4$. Here, the optimal approximation order with respect to the L^2 (left) and H^2 (right) norm is reached for $\varepsilon = C \cdot h^k$ for $k = 2,3$, but neither for $k \leq 1$ nor for $k \geq 4$, see Figure 9. Finally, the optimal approximation order for $p = 5$ with respect to the L^2 (left) and H^2 (right) norm is reached for $\varepsilon = C \cdot h^k$ for $k = 3$, but neither for $k \leq 2$ nor for $k \geq 4$, as shown in Figure 10.

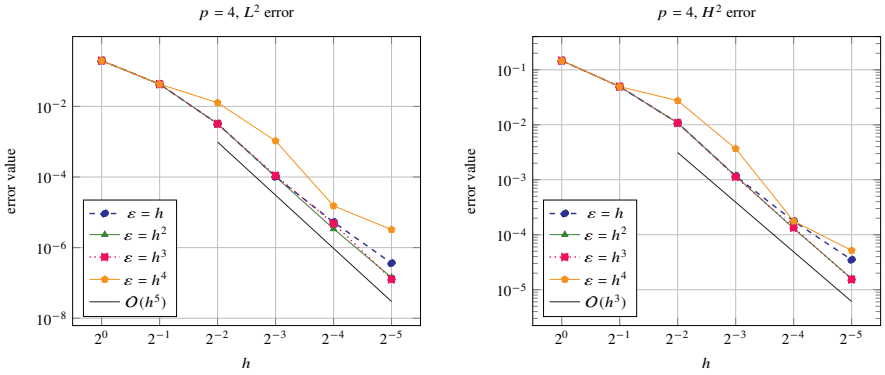

Fig. 9 Biharmonic equation (25): Relative L^2 (left) and H^2 (right) errors of the approximate solution for basis functions of degree four in $\hat{G}_h^{1,\varepsilon}$ for four choices of ε.

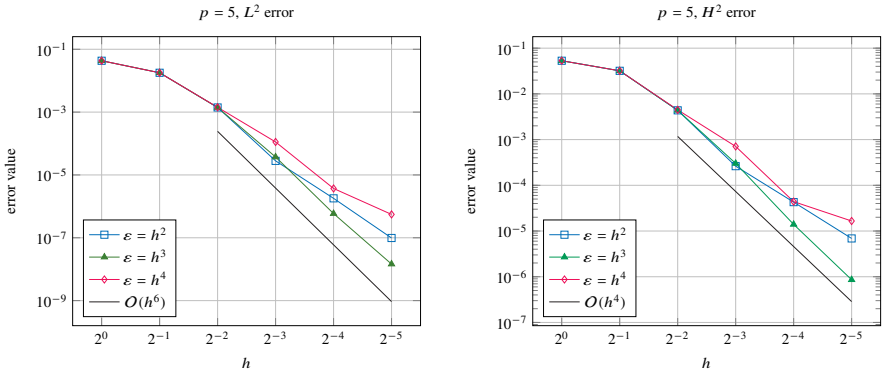

Fig. 10 Biharmonic equation (25): Relative L^2 (left) and H^2 (right) errors of the numeric solution for basis functions of degree five in $\hat{G}_h^{1,\varepsilon}$ for three choices of ε.

On the one hand, a higher power of h and thus a smaller value of ε results in smoother, but at the same time in fewer basis functions, hence in a loss of approximation power. On the other hand, while choosing a larger value of ε increases the dimension of $\hat{G}_h^{1,\varepsilon}$, the resulting discretizations are not smooth enough for solving higher order problems. We conjecture that $\varepsilon = C \cdot h^{p-2}$ is the optimal choice.

5.2 Dimension of the Space

We investigate the influence of ε on the number of interface basis functions, and thus on the dimension of the space $\hat{G}_h^{1,\varepsilon}$. Note that the number of trivially smooth basis functions is not affected by the choice of ε.

We cannot expect nested spaces, i.e., we cannot ensure that

$$\hat{G}_h^{1,\varepsilon} \subseteq \hat{G}_{\frac{h}{2}}^{1,\varepsilon}.$$

Nevertheless, the number of interface basis functions grows as h is decreased.

Figure 11 shows the number of interface basis functions for different degrees and different choices of ε. For $\varepsilon = C \cdot h^k$ with $k \leq p-2$, the number of interface basis functions grows linearly under h-refinement for all degrees. A larger choice of k, however, results in significantly fewer functions.

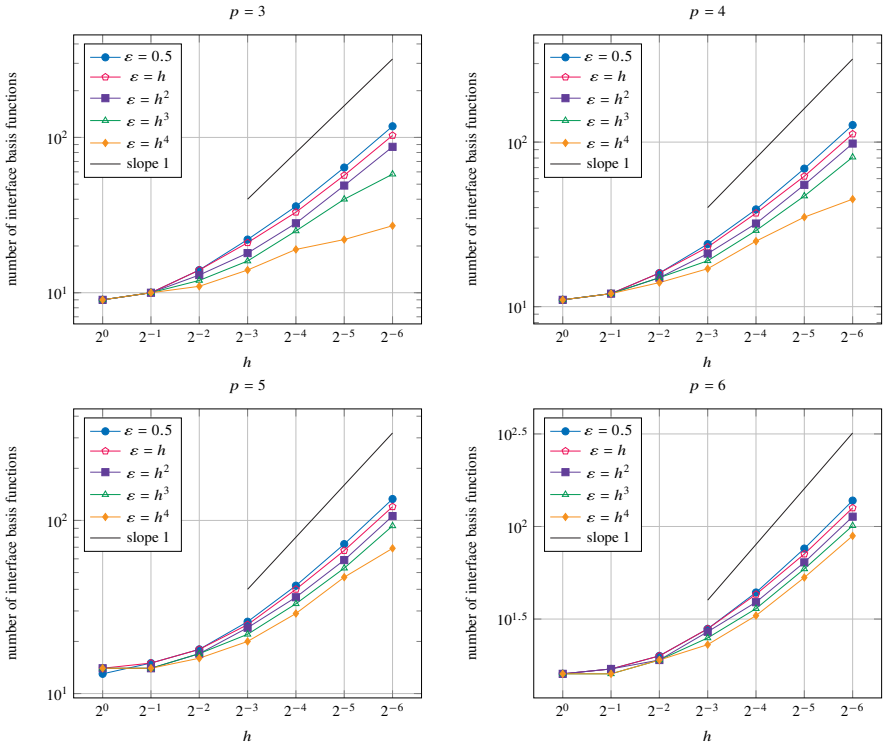

Fig. 11 Number of interface basis functions under uniform h-refinement on the domain shown in Figure 1. Basis functions of degree three (top left), four (top right), five (bottom left) and six (bottom right) for various choices of ε.

6 Conclusion

We proposed a concept of constructing approximately C^1-smooth isogeometric functions on planar multi-patch domains which is based on selecting eigenvalues and corresponding eigenvectors of the matrix representation of a suitable bilinear form. The functions will have a non-zero gradient jump across the interface.

We studied two different bilinear forms. The first bilinear form led to a bound on the gradient jump of the form

$$\|[\nabla f]\|^2_{L^2(\Gamma)} \leq \varepsilon \|f\|^2_{L^2(\Omega)},$$

where ε is to be chosen in advance. This bound is h-independent. However, the space constructed via this bilinear form does not necessarily contain trivially smooth functions, which led to a decrease in the approximation order. The function space based on the second bilinear form contains all trivially smooth isogeometric functions and the gradient jump is bounded by a mesh-dependent term.

Numerical experiments suggested that for second-order problems, the latter approach maintains the optimal approximation order even for constant choices of ε and that the functions are sufficiently smooth to solve the biharmonic equation. The convergence of the approximate solution was influenced by the choice of ε. Depending on the degree of the basis functions, ε had to be chosen as a suitable power of the mesh size h in order to achieve convergence of the solution to the biharmonic problem.

In future work we would like to establish a theoretical background for the experimental results. This includes

- investigating a projector to the space of approximately C^1-smooth isogeometric functions to prove optimal convergence rates,
- studying the eigenstructure of the matrix Q to develop a lower bound for the number of non-trivial basis functions and
- analyzing the influence of ε.

The last point affects the first two points as well: A smaller value of ε creates smoother but fewer functions. Last but not least we are interested in generalizing the approach to domains with more than two patches and to the three-dimensional case.

References

1. Y. Bazilevs, L. B. de Veiga, J. A. Cottrell, T. J. Hughes, and G. Sangalli. Isogeometric analysis: Approximation, stability and error estimates for h-refined meshes. *Mathematical Models and Methods in Applied Sciences*, 16:1031 – 1090, 2006.
2. C. Bernardi, Y. Maday, and F. Rapetti. Basics and some applications of the mortar element method. *GAMM-Mitteilungen*, 28(2):97–123, 2005.
3. E. Brivadis, A. Buffa, B. Wohlmuth, and L. Wunderlich. Isogeometric mortar methods. *Computer Methods in Applied Mechanics and Engineering*, 284:292–319, 2015.
4. C. L. Chan, C. Anitescu, and T. Rabczuk. Isogeometric analysis with strong multipatch C^1-coupling. *Computer Aided Geometric Design*, 62:294 – 310, 2018.
5. A. Collin, G. Sangalli, and T. Takacs. Analysis-suitable G^1 multi-patch parametrizations for C^1 isogeometric spaces. *Computer Aided Geometric Design*, 47:93 – 113, 2016.
6. J. A. Cottrell, T. J. R. Hughes, and Y. Bazilevs. *Isogeometric Analysis. Toward Integration of CAD and FEA*. John Wiley and Sons, Chichester, England, 2009.
7. D. Groisser and J. Peters. Matched G^k-constructions always yield C^k-continuous isogeometric elements. *Computer Aided Design*, 34:67–72, 2015.
8. C. Grossmann. Penalties, Lagrange multipliers and Nitsche mortaring. *Differential Inclusions, Control and Optimization*, 20:205–220, 2010.
9. M. Kapl, F. Buchegger, M. Bercovier, and B. Jüttler. Isogeometric analysis with geometrically continuous functions on planar multi-patch geometries. *Computer Methods in Applied Mechanics and Engineering*, 316:209 – 234, 2017.
10. M. Kapl, G. Sangalli, and T. Takacs. Dimension and basis construction for analysis-suitable G^1 two-patch parameterizations. *Computer Aided Geometric Design*, 52:75 – 89, 2017.
11. M. Kapl and V. Vitrih. Space of C^2-smooth geometrically continuous isogeometric functions on planar multi-patch geometries: Dimension and numerical experiments. *Computers & Mathematics with Applications*, 73:2319 – 2338, 2017.

12. M. Kapl and V. Vitrih. Space of C^2-smooth geometrically continuous isogeometric functions on two-patch geometries. *Computers & Mathematics with Applications*, 73(1):37 – 59, 2017.
13. M. Kapl and V. Vitrih. Dimension and basis construction for C^2-smooth isogeometric spline spaces over bilinear-like G^2 two-patch parameterizations. *Journal of Computational and Applied Mathematics*, 335:289 – 311, 2018.
14. M. Kapl, V. Vitrih, B. Jüttler, and K. Birner. Isogeometric analysis with geometrically continuous functions on two-patch geometries. *Computers & Mathematics with Applications*, 70(7):1518 – 1538, 2015.
15. U. Langer and I. Toulopoulos. Analysis of multipatch discontinuous Galerkin IgA approximations to elliptic boundary value problems. *Comp. Visual. Science*, 17(5):217–233, 2016.
16. V. P. Nguyen, P. Kerfriden, M. Brino, S. P. Bordas, and E. Bonisoli. Nitsche's method for two and three dimensional NURBS patch coupling. *Computational Mechanics*, 53(6):1163–1182, 2014.
17. B. Rivière. *Discontinuous Galerkin Methods for Solving Elliptic and Parabolic Equations: Theory and Implementation*. SIAM, 2008.
18. L. L. Schumaker. *Spline Functions: Basic Theory*. Wiley, New York, 1981.
19. M. F. Wheeler. An elliptic collocation-finite element method with interior penalties. *SIAM Journal on Numerical Analysis*, 15(1):152–161, 1978.